Supplementary material on

‘Steady axial electric field may lead to controllable cross-stream migration of droplets in confined oscillatory microflows’

Somnath Santra and Suman Chakraborty

Department of Mechanical Engineering, Indian Institute of Technology Kharagpur,

Kharagpur – 721302, India

S1. Numerical implementation

The governing equations have been solved using the finite element method taking the appropriate boundary conditions into consideration. Due to the complex nature of the coupled, nonlinear, partial differential governing equations, for efficient execution of the computational approach, we have used the foundation of Comsol Multiphysics software (Mandal et al. 2015; Sáenz et al. 2017; Santra et al. 2019; Zang et al. 2018; Chubynsky et al. 2020; Kaplan & Mahadevan 2015; Wang et al. 2019), and have incorporated additional user-defined routines to capture the detailed physics. As an essential premise of our computation, we have employed the in-built laminar flow interface that uses a finite element solver for the governing Navier-Stokes equation. Newton iterations are executed and the MUMPS solver has been implemented for the linear algebraic system deriving from the finite-element formulation. For temporal discretization, we have employed a Second-order BDF (backward differentiation formula) scheme with free steps. For accurately capturing the dynamics of the droplet, in this time-stepping method, we have chosen the maximum time step having a value of 5×10^{-4} whereas the numerical simulation starts at a very small time step having an order of 10^{-7}. In all simulations, we have fixed a tolerance level of 10^{-6}. For the post-processing of the numerical data, we have used our in-house Matlab code. For confirming the accuracy of the results, we have validated the numerical results extensively with the well-established numerical and experimental results as reported in the literature, and found an excellent agreement.

For tracking the interface, we have adopted phase field model and coupled it with the Navier-Stokes equation through the phase-field parameter-dependent physical properties and interfacial tension. Further to this, we have accommodated the electrical forcing and interfacial tension as functions of phase field parameter and incorporated in the governing Navier-Stokes equation as forcing terms. In addition, we have also expressed the electrophysical properties as a function of the phase field order parameter. In this way, we have developed a customized complete electrohydrodynamic model for multiphase and multicomponent flows in the skeletal structure provided by the Software.

S2. Grid independence study and Cahn number independence study.

In the phase field method, Cahn number ($Cn = \xi^* / H^*$, where the thickness of the interface is controlled by the parameter ξ^*) is used to represent the thickness of the interfacial region, which in turn alters the dynamics of the droplet. However, below a particular value of *Cn*, the dynamics becomes independent of the same. Hence, we need to perform the Cahn number independence

† E-mail address for correspondence: suman@mech.iitkgp.ernet.in

test. Again, for properly resolving the interfacial properties, one needs to employ adequately fine meshes at the interfacial region (Yue et al. 2010; Zhou et al. 2010). Thus, the grid size is also found to be related to Cahn number. For the Cahn number independence test, we have assumed the Cahn number to be the same as that of the grid size in the computational domain (Santra et al. 2018; Mandal et al. 2015; Santra et al. 2020). Therefore, the Cahn number independence study automatically ensures the grid independence study and vice versa. For the Cahn number independence test, we have considered *Cn* = 0.015, 0.01, 0.005 as depicted in figure S1(a). The figure shows negligible variation among the results for lower values of *Cn*. Again, a too-small value of *Cn* (=0.005) unnecessarily enhances the computational cost. Hence, we have chosen *Cn*=0.01 in the present analysis.

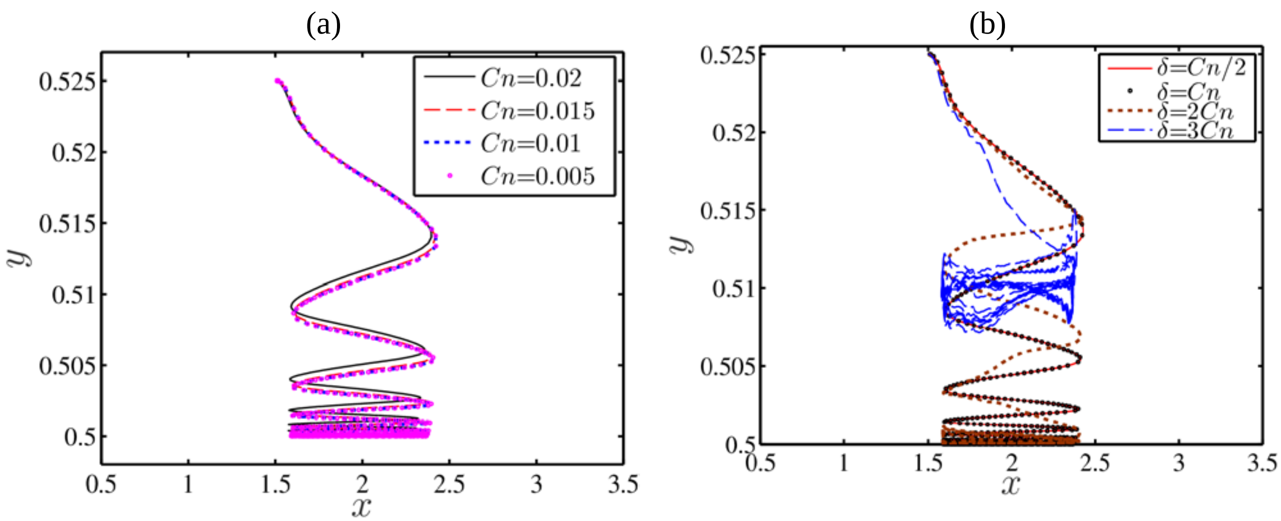

FIGURE S1. (a) Cahn number independence study. (b) Effect of the grid size on the migration characteristic of the droplet in combined presence of axial electric field and background oscillatory flow. Important parameters are S=2, R=0.5, Ca=0.3, Re=0.1, a=0.3,Y_d=0.525, ρ_r=1, λ=1and Ca_E=1.5.

It is worth mentioning that, for *Cn*=0.01, the thin interface between two immiscible phases encounters a large gradient of the order parameter. To tackle this, very fine mesh is required at the interfacial region. If we chose coarse grids in the computational domain, especially near the interface, it creates a poor implementation of interfacial tension, which can develop spurious oscillations in the solution, especially near the interfacial region (Yue et al. 2004). Because of that, the results may vary unphysically, which is not desirable in numerical modeling of any realistic scenario. To explicitly demonstrate the importance of optimal grid size (δ) compared to interfacial thickness (*Cn*), we further performed another set of studies, where we fixed the value of *Cn*=0.01 and varied the size of the grid element as depicted in figure S1(b). The figure clearly demonstrates that the migration characteristic is extremely sensitive to mesh size and a coarser mesh creates incorrect prediction of the oscillatory migration characteristic. However, below a particular value of the grid size (δ=*Cn*), a negligible discrepancy is observed in the migration characteristic and it becomes independent of the size of the grid element. We have taken *Cn*=0.01 and δ=0.01 into the numerical analysis and we have found an excellent quantitive matching with benchmark results reported in the literature.

References

CHUBYNSKY, M. V., BELOUSOV, K.I., LOCKERBY, D.A. & SPRITTLES, J.E. 2020 Bouncing off the Walls: The Influence of Gas-Kinetic and van der Waals Effects in Drop Impact. *Phys. Rev. Lett.* **124**(8), 084501.

KAPLAN, C.N. & MAHADEVAN, L. 2015 Evaporation-driven ring and film deposition from colloidal droplets. *J. Fluid Mech.* **781**, R2.

MANDAL, S., GHOSH, U., BANDOPADHYAY, A. & CHAKRABORTY, S. 2015 Electro-osmosis of superimposed fluids in the presence of modulated charged surfaces in narrow confinements. *J. Fluid Mech.* **776**(May), 390–429.

SÁENZ, P.J., WRAY, A.W., CHE, Z., MATAR, O.K., VALLURI, P., KIM, J. & SEFIANE, K. 2017 Dynamics and universal scaling law in geometrically-controlled sessile drop evaporation. *Nat. Commun.* **8**(1), 14783.

SANTRA, S., DAS, S. & CHAKRABORTY, S. 2020 Electrically modulated dynamics of a compound droplet in a confined microfluidic environment. *J. Fluid Mech.* **882**, A23.

SANTRA, S., MANDAL, S. & CHAKRABORTY, S. 2019 Confinement effect on electrically induced dynamics of a droplet in shear flow. *Phys. Rev. E* **100**(3), 33101.

SANTRA, S., MANDAL, S. & CHAKRABORTY, S. 2018 Electrohydrodynamics of confined two-dimensional liquid droplets in uniform electric field. *Phys. Fluids* **30**(6), 62003.

SANTRA, S., PANIGRAHI, D.P., DAS, S. & CHAKRABORTY, S. 2020 Shape evolution of compound droplet in combined presence of electric field and extensional flow. *Phys. Rev. Fluids* **5**(6), 63602.

WANG, Q., JONES, A.-A.D., GRALNICK, J.A., LIN, L. & BUIE, C.R. 2019 Microfluidic dielectrophoresis illuminates the relationship between microbial cell envelope polarizability and electrochemical activity. *Sci. Adv.* **5**(1), 1-11.

YUE, P., FENG, J.J., LIU, C. & SHEN, J. 2004 A diffuse-interface method for simulating two-phase flows of complex fluids. *J. Fluid Mech.* **515**, 293–317.

YUE, P., ZHOU, C. & FENG, J.J. 2010 Sharp-interface limit of the Cahn–Hilliard model for moving contact lines. *J. Fluid Mech.* **645**, 279–294.

ZANG, D., LI, L., DI, W., ZHANG, Z., DING, C., CHEN, Z., SHEN, W., BINKS, B.P. & GENG, X. 2018 Inducing drop to bubble transformation via resonance in ultrasound. *Nat. Commun.* **9**(1), 3546.

ZHOU, C., YUE, P., FENG, J.J., OLLIVIER-GOOCH, C.F. & HU, H.H. 2010 3D phase-field simulations of interfacial dynamics in Newtonian and viscoelastic fluids. *J. Comput. Phys.* **229**(2), 498–511.